Use of Electrical Insulation in Lithium-Cooled Fusion Reactor Blankets

D.K. Sze and W.E. Stewart

April 1974

UWFDM-99

Presented at the 1st Topical Meeting on the Technology of Controlled Nuclear Fusion, San Diego CA, 14-18 April 1974.

FUSION TECHNOLOGY INSTITUTE

UNIVERSITY OF WISCONSIN

MADISON WISCONSIN

Use of Electrical Insulation in Lithium-Cooled Fusion Reactor Blankets

D.K. Sze and W.E. Stewart

Fusion Technology Institute
University of Wisconsin
1500 Engineering Drive
Madison, WI 53706

http://fti.neep.wisc.edu

April 1974

UWFDM-99

Presented at the 1st Topical Meeting on the Technology of Controlled Nuclear Fusion, San Diego CA, 14-18 April 1974.

Use of Electrical Insulation in Lithium-Cooled Fusion Reactor Blankets

Dai-Kai Sze and Warren E. Stewart

Departments of Nuclear and Chemical Engineering
University of Wisconsin
Madison, Wisconsin 53706

FDM 99

Paper presented at the First Topical Meeting on the Technology of Controlled Nuclear Fusion held in San Diego - April 14-18, 1974.

Use of Electrical Insulation in Lithium-Cooled Fusion Reactor Blankets

Dai-Kai Sze and Warren E. Stewart
Departments of Nuclear and Chemical Engineering
Wisconsin Fusion Feasibility Study Group
University of Wisconsin
Madison, Wisconsin

Abstract

The performance of lithium-cooled fusion reactor blankets can be substantially improved if electrical insulators can be used. Plant efficiencies can be increased, wall stresses can be reduced, and higher wall loadings and magnetic fields can be employed. Case studies are given for a Tokamak reactor to show the improvement attainable as a function of the operating conditions permitted for the insulating material.

Introduction

Lithium is a desirable coolant and breeding material for fusion reactor blankets. Its nuclear properties are ideal and its thermal conductivity is high. The main disadvantage of litium is a high electrical conductivity, which leads to added pressure gradients in flow across magnetic fields. Suppression of turbulence also occurs in magnetic fields, and heat transfer is thus retarded, but this is a minor effect in lithium because of its very low Prandtl number (Pr = 0.03 at 500°C). The added pressure gradient, however, has been a major deterrent to use of lithium cooling in fusion reactor designs.

Reasonable pressure drops can be obtained in lithium-cooled blankets by a careful choice of flow arrangement. Low velocities must be used, expecially when moving the lithium at an angle to the magnetic field. Our previous paper (1) describes such a blanket, designed for the Tokomak system UWMAK-1 (2). The design requirements are given in Table I, and the main results are shown in the first column of Table II. The pumping power (27MW) is relatively small, and the maximum wall stress, (13,500 psi) is tolerable. However, the wall stress would become a problem if a higher coolant flow or magnetic field were desired, or if a structural material with higher electrical conductivity were substituted for the stainless steel.

It is well known (3) that insulated walls can be used to reduce magnetohydrodynamic pressure drops. In our previous designs (1, 4) no insulators were used except in the feed and discharge pipes, where the radiation intensity is low. This restriction was imposed for lack of information about effects of nuclear radiation on insulating materials.

Although proven insulators remain to be developed; it is useful to see what effects they would have on blanket performance. The likelihood of successful development depends on the conditions of exposure; hence we have considered the following four possibilities:

0. No insulation.
1. Insulation used; can stand moderate radiation but has to be shielded from lithium.
2. Insulation used; can stand strong radiation but has to be shielded from lithium.
3. Insulation used; can stand strong radiation and exposure to flowing lithium.

Magnetohydrodynamic Pressure Drops

The combination of high magnetic field and electrically conducting coolant specified in Table 1 causes the flow to remain laminar throughout the blanket for all feasible coolant velocities. The pressure drops can accordingly be estimated by the methods described by Hoffman and Carlson (5) for laminar magnetohydrodynamic flows. We follow their conservative procedure of estimating the total pressure drop as the sum of the Hartmann (developed flow) losses and the entrance and exit effects.

For a fully-developed laminar flow between parallel plates with a uniform transverse magnetic field perpendicular to the plates, the Hartmann pressure gradient is given by the following equation (6)

$$-\frac{dp}{dx} = \frac{\mu v}{a^2}\left[\frac{H_\perp^2 \tanh H_\perp}{H_\perp - \tanh H_\perp} + \frac{H_\perp^2 C}{1+C}\right] \qquad (1)$$

where $H_\perp$ = transverse Hartmann number $\equiv a B_\perp \sqrt{\sigma/\mu}$

$B_\perp$ = transverse magnetic field

μ = fluid viscosity

v = mean velocity

C = wall conductance ratio = $\frac{\sigma_w t_w}{\sigma a}$

a = channel half-width

σ = electrical conductivity of fluid

σ_w = electrical conductivity of wall material

t_w = wall thickness

For a non-conducting wall and high Hartmann number, Equation ([1]) gives:

$$-\frac{dP}{dx} \doteq \frac{B_\perp v}{a^2}\sqrt{\sigma\mu}\left\{\begin{array}{l} H_\perp >> 1 \\ C << 1/H_\perp \end{array}\right\} \qquad (2)$$

For a conducting wall and high Hartmann number, the last term of Eq. 1 dominates, giving

$$-\frac{dp}{dx} = \frac{vB_\perp^2 \sigma_w t_w}{a(1+C)} \qquad \{H_\perp >> 1 + C^{-1}\} \qquad (3)$$

Equations (2) and (3) can be extended to rectangular and circular ducts, by redefining a as the mean half-width of flow cross section in the direction of B . This extension agrees closely with Hoffman and Carlson's empirical expressions for rectangular and circular ducts, in the limit of large Hartmann number. For a tube of inside diameter D, we obtain $a = \pi D/8$.

The entrance and exit effects are caused by variations of $[\underline{v} \times \underline{B}]$ along the flow direction. The resulting pressure drops are estimated here by the equation

$$\Delta p = K_{p1E} \frac{\sigma(b_1 + b_2)}{(v_1 + v_2)} \left|\Delta(v B_\perp)^2\right| \qquad (4)$$

obtained by approximate integration of the magnetohydrodynamic equations. Here v_1 and v_2 and the initial and final cross-section mean velocities, and b_1 and b_2 are the corresponding mean half-widths taken normal to B .

The coefficient K_{p1E} is estimated here from Hoffman and Carlson's Eq. (16), derived for a linear change of magnetic field over a downstream length L_F:

$$K_{p1E} = \sum_i f_i \frac{b}{L_F}\left\{1 - \frac{b}{k_i L_F}\left[1 - e^{-k_i L_F/b}\right]\right\} \qquad (5)$$

Here the coefficients f_i are given by

$$f_i = \frac{4 \sin k_i}{k_i^3}\left[\frac{\sin k_i - k_i \cos k_i}{2k_i - \sin 2k_i}\right] \qquad (6)$$

and the k_i are the roots of the equation

$$C k_i \tan k_i = 1 \qquad (7)$$

The end-of-loop pressure drop increases strongly with the channel width b, since K_{plE} increases with b. This behavior is contrary to that of ordinary flows, and is exploited in the designs given below.

Equations (1)-(3) and (5)-(7) were developed for systems with homogeneous walls. They also hold for laminated walls, if the first or second layer on the fluid side is a good electrical insulator.

System Description

The coolant flow scheme for these case studies is shown on Fig. 1 and 2. The structural material is 316 stainless steel. To limit corrosion, a temperature limit of 500°C is imposed on the surfaces wetted by the lithium. A corrosion allowance of 0.015 mm/year, based on the data of Gill (7), is included in initial wall thickness. The inner 20 cm of the blanket is designed for a life of 2 years, while the rest of the reactor is designed for 30 years.

The reactor has 12 independent modules, one for each magnet. Each module has four blanket unites; one between the divertors and reactor axis, and three for the rest of the perimeter. Tube bundles are used for coolant supply and discharge, to reduce end-of-loop pressure drops. Each bundle is connected to a toroidal header running parallel to the main magnetic field. Each toroidal header opens into a set of poloidal headers, connected in turn to the radial-flow cells that form the first wall.

Design Modifications

Table II summarizes the special features of the various blanket designs, in comparison with the blanket of UWMAK-1.

Design 0 uses no insulation. The protected insulation used in UWMAK-1 is removed. The feed and discharge bundles are changed to sixteen 0.25 m I.D. tubes in place of the four 0.5 m I.D. tubes used in UWMAK-1. The latter change reduces the end-of-loop pressure drop, with very little effect on the Hartmann loss; this feature is also used in the following designs.

Design 1 uses insulation in the feed and discharge tubes. The insulation is protected from contact with the lithium by 0.5 mm of stainless steel. A heavier covering (2 mm) was used in UWMAK-1, but 0.5 mm is now considered adequate.

Design 2 uses an insulation with better radiation tolerance, and adds insulated turning vanes at the junctions of the toroidal and poloidal headers to reduce the end-of-loop pressure drops. The poloidal header walls are also insulated. All insulation is protected by 0.5 mm of stainless steel.

Design 3 is like Design 2, except that it uses an insulation that can stand exposure to flowing lithium. The stainless steel protection is, therefore, eliminated with a corresponding reduction of pressure drop.

Comparison of Results

The main results of the designs are compared in Table II. Detailed calculations for the unit nearest the machine axis are given in Table III. The temperature distributions are the same for all the designs and are obtainable from Reference (1).

Designs 1, 2, and 3 give significantly smaller pressure drops than Design 0 and UWMAK-1. The maximum pressure, maximum wall stress, and pumping power are also significantly reduced. The greatest improvement occurs on insulating the poloidal headers; compare Designs 1 and 2 in Table 3.

Table IV gives detailed results for all blanket units of Design 2, a probable limit of insulator development. Figure 3 gives the pressure distribution in this design for the unit nearest the machine axis.

Discussion

Several alternatives exist for improving the plant performance when insulated walls are used. For example, instead of reducing the pressure in the blanket, we could circulate more coolant and raise the coolant inlet temperature, thus improving the external power cycle efficience. The pumping power consumption also increases with the flow rate, so that an optimum temperature rise exists, which is smaller for an insulated blanket.

The external efficiency is illustrated in Figure 4 for a Carnot cycle with a fixed heat input at the mean coolant temperature and with heat rejection at 100°C. Tripling the coolant flow in Design 2 reduces the temperature rise from 200°C to 67°C and raises the Carnot efficiency by 5%, giving 250 MW additional power generated. Deducting the pumping power, which increases ninefold, we get a net gain of 186 MW. Even after this increase in flow rate, the wall stresses are lower than in UWMAK-1.

Insulation would also extend the feasible range of lithium cooling to higher magnetic fields, higher wall loadings, and to structural materials with higher electrical conductivities. Research on insulators for fusion reactor blankets should, therefore, be given high priority.

References

1. Sze, D. K., and W. E. Stewart, "Thermal and Mechanical Design Considerations for Lithium-Cooled Tokamak Reactor Blankets," Fifty Symposium on Engineering Problems of Fusion Research, Princeton, N.J., 1973.
2. Kulcinski, G. L., "UWMAK-1, A. Wisconsin Fusion Reactor Design", IAEA Workshop on Fusion Reactor Design Problems, Culham, England, 1974.
3. Carlson, G. A., and M. A. Hoffman, "Effect on Magnetic Fields on Heat Pipes," USAEC Report UCRL-72060, 1970.
4. Sze, D.K., and W.E. Stewart," Lithium Cooling for a Low-β Tokamak Reactor," Texas Symposium on the Technology of Controlled Thermonuclear Fusion Experiments and the Engineering Aspects of Fusion Reactors, 1972.
5. Hoffman, M.A., and G.A. Carlson, "Calculating Techniques for Estimating the Pressure Losses for Conducting Fluid Flows in Magnetic Field," USAEC Report UCRL-51010, 1971.
6. Sutton, G.W., and A. Sherman," Engineering Magnetohydrodynamics," McGraw Hill, N.Y., 1956.
7. Gill, W.N., R.P. Vanek, R.V. Jelinek and C.S. Grove, Jr., "Mass Transfer in Liquid-Lithium System," AIChE Journal, 6, 193 (1960).

Table I

SUMMARY OF DESIGN SPECIFICATIONS

Total Thermal Load	5000 MW
Major Radius	13 m
Minor Radius	5.5 m
Thermal Wall Loading	1.77 MW/m^2
Magnetic Field on Plasma Axis	3.86 Tesla
Structural Material	316 SS
Blanket Coolant	Lithium
Maximum Lithium Temperature	500°C
Lithium Temperature Rise	200°C
Lithium Flow Rate	5.64×10^3 kg/sec

Table II

COMPARISON OF BLANKET DESIGNS

	UWMAK-1	Design 0	Design 1	Design 2	Design 3
Feed and Discharge Tube Bundles:					
Number of tubes	4	16	16	16	16
Inside diameter	0.5 m	0.25 m	0.25 m	0.25 m	0.25 m
Insulation	Yes	No	Yes	Yes	Yes
Protector thickness	2.0 mm	-	0.5 mm	0.5 mm	None
Turning Vanes at Header Junctions	None	None	None	Insulated, 0.5 mm protector	Insulated
Poloidal Headers:					
Insulation	No	No	No	Yes	Yes
Protector thickness	-	-	-	0.5 mm	None
Blanket Performance					
Δp, unit nearest axis, psi	507*	506	434	148	100
Maximum pressure on first wall, psia	380*	379	343	105	64
Maximum tensile stress in first wall, psi	13,500*	13,400	12,500	7,000	5,000
Total power required for pumping, MW	27*	27	23	8	5

*New values based on revised calculation of entrance and exit effect at header junctions.

Table III

SUMMARY OF PRESSURE DROP CALCULATIONS FOR THE UNIT NEAREST THE MACHINE AXIS

	v,m/sec	a,m	b,m	$L_{F/b}$	K_{plE}	t_w,mm	L,m	$B_\perp$,Tesla	Pressure drops*, psi Δp_E	Δp_H	Total
Design 0											
Feed or discharge tubes	0.1	0.098	0.098	10.2	0.032	4.5	1.83	5.9	4.0	40.5	44.5×2
Junction of tubes with toroidal header	0.1	-	0.098	1.0	0.16	-	-	5.9	19.8	-	19.8×2
Toroidal header	0.705	0.196	-	-	-	9.0	3.4	0.6	-	3.2	3.2
Poloidal header	0.083	0.10	0.25	1.0	0.16	3.5	16.0	6.5	50.8×2	270.2	371.8
Radial cells	0.038	0.5	-	-	-	3.0	1.6	6.5	-	2.1	2.1
											505.7
Design 1											
Feed or discharge tubes	0.1	0.098	0.098	10.2	0.032	0.5	1.83	5.9	4.0	4.5	8.5×2
Junction of tubes with toroidal header	0.1	-	0.098	1.0	0.16	-	-	5.9	19.8	-	19.8×2
Toroidal header	0.705	0.196	-	-	-	9.0	3.4	0.6	-	3.2	3.2
Poloidal header	0.083	0.10	0.25	1.0	0.16	3.5	16.0	6.5	50.8×2	270.2	371.8
Radial cells	0.038	0.5	-	-	-	3.0	1.6	6.5	-	2.1	2.1
											433.7
Design 2											
Feed or discharge tubes	0.1	0.098	0.098	10.2	0.032	0.5	1.83	5.9	4.0	4.5	8.5×2
Junction of tubes with toroidal header	0.1	-	0.098	1.0	0.16	0.5	-	5.9	19.8	-	19.8×2
Toroidal header	0.705	0.196	-	-	-	0.5	3.4	0.6	-	0.0	0.0
Poloidal header	0.083	0.10	0.125	1.0	0.16	0.5	16.0	6.5	25.4×2	38.6	89.4
Radial cells	0.038	0.5	-	-	-	3.0	1.6	6.5	-	2.1	2.1
											148.1

Table III (continued)

SUMMARY OF PRESSURE DROP CALCULATIONS FOR THE UNIT NEAREST THE MACHINE AXIS

	v,m/sec	a,m	b,m	$L_{F/b}$	K_{plE}	t_w,mm	L,m	$B_\perp$,Tesla	Pressure drops*, psi Δp_E	Δp_H	Total
Design 3											
Feed or discharge tubes	0.1	0.098	0.098	10.2	0.032	0	1.83	5.9	4.0	0.0	4.0×2
Junction of tubes with toroidal header	0.1	-	0.098	1.0	0.16	0	-	5.9	19.8	-	19.8×2
Toroidal header	0.705	0.196	-	-	-	0	3.4	0.6	-	0.0	0.0
Poloidal header	0.083	0.10	0.125	1.0	0.16	0	16.0	6.5	25.4×2	0.0	50.8
Radial cells	0.038	0.5	-	-	-	3.0	1.6	6.5	-	2.1	2.1
											100.5

* E = Entrance or Exit; H = Hartmann

Table IV

SUMMARY OF PRESSURE DROP CALCULATIONS FOR DESIGN 2

	v,m/sec	a,m	b,m	$L_{F/b}$	K_{plE}	t_w,mm	L,m	$B_\perp$,Tesla	Pressure drops, psi Δp_E	Δp_H	Total
For unit nearest reactor axis											
Feed or discharge tubes	0.1	0.098	0.098	10.2	0.032	0.5	1.83	5.9	4.0	4.5	8.5×2
Junction of tubes with toroidal header	0.1	-	0.098	1.0	0.16	0.5	-	5.9	19.8	-	19.8×2
Toroidal header	0.705	0.196	-	-	-	0.5	3.4	0.6	-	0.0	0.0
Poloidal header	0.083	0.10	0.125	1.0	0.16	0.5	16.0	6.5	25.4×2	38.6	89.4
Radial cells	0.038	0.5	-	-	-	3.0	1.6	6.5	-	2.1	2.1
											148.1
For units on top and bottom of the torus											
Feed tubes	0.235	0.098	0.098	10.2	0.032	0.5	8.0	3.9	4.1	20.0	24.1
Entry from tubes to toroidal header	0.235	-	0.098	1.0	0.16	0.5	-	3.9	20.3	-	20.3
Toroidal header	0.939	0.196	-	-	-	0.5	6.8	0.5	-	0.0	0.0
Poloidal header	0.092	0.10	0.125	1.0	0.16	0.5	8.0	4.2	11.8×2	8.9	32.5
Radial cells	0.038	0.5	-	-	-	3.0	1.6	5.0	-	1.3	1.3
Exit from toroidal header to tubes	0.235	-	0.098	1.0	0.16	0.5	-	2.64	9.3	-	9.3
Discharge tubes	0.235	0.098	0.098	10.2	0.032	0.5	5.0	2.64	1.9	5.7	7.6
											95.1

Table IV (continued)

SUMMARY OF PRESSURE DROP CALCULATIONS FOR DESIGN 2

	v,m/sec	a,m	b,m	$L_{F/b}$	K_{plE}	t_w,mm	L,m	$B_\perp$,Tesla	Pressure drops, psi Δp_E	Δp_H	Total
					For units farthest from reactor axis						
Feed or discharge tubes	0.235	0.098	0.098	5.1	0.032	0.5	5.0	2.6	1.9	5.7	7.2×2
Junction of tubes with toroidal header	0.235	-	0.098	1.0	0.16	0.5	-	2.6	9.3	-	9.3×2
Toroidal header	0.939	0.196	-	-	-	0.5	6.8	0.3	-	0.0	0.0
Poloidal header	0.092	0.10	0.125	1.0	0.16	0.5	8.0	2.6	4.5×2	3.4	12.4
Radial cells	0.038	0.5	-	-	-	3.0	1.6	2.6	-	0.5	0.5
											45.9

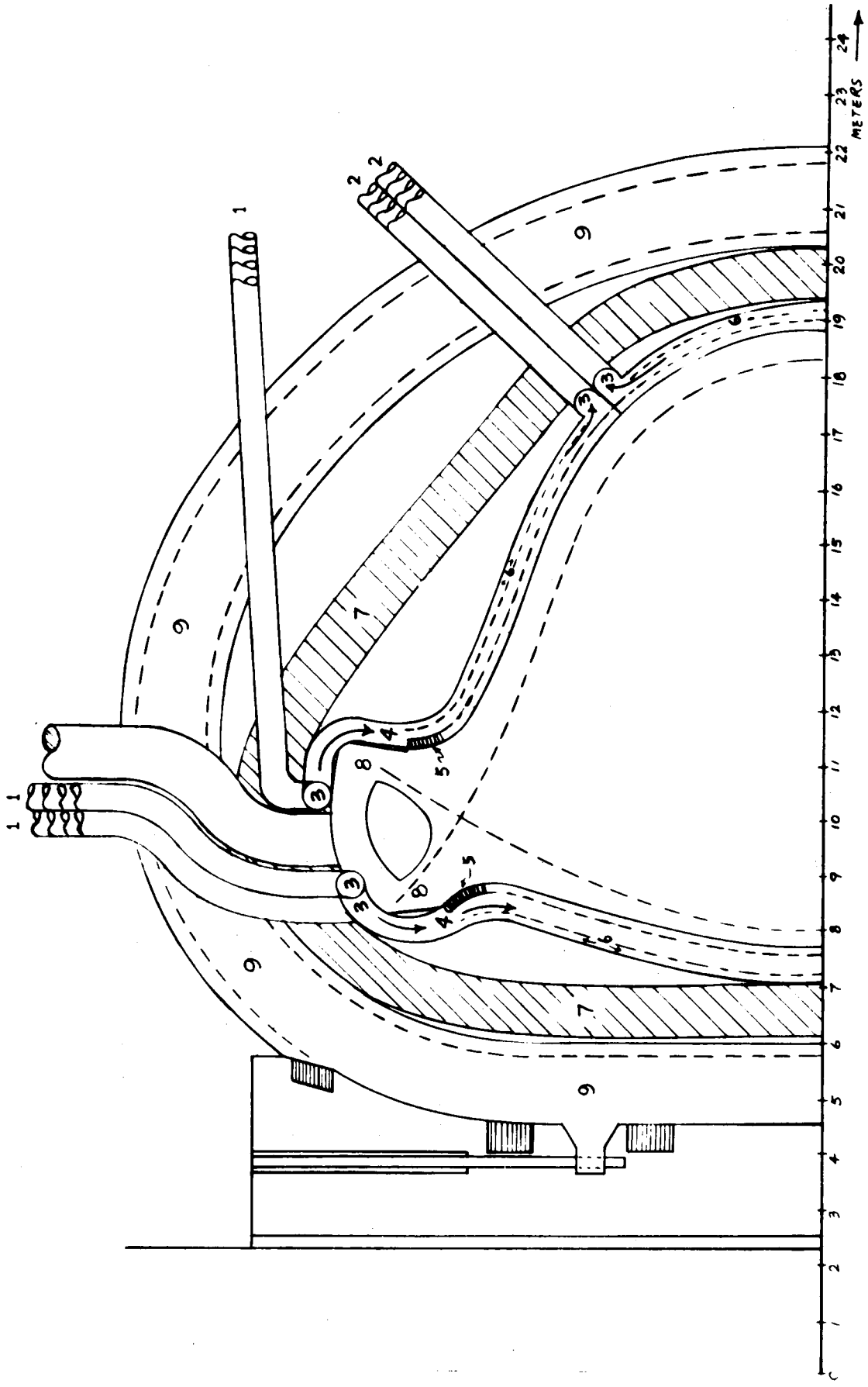

FIGURE 1 SECTION VIEW OF A TOROIDAL MODULE

1. Feed Pipes
2. Discharge Pipes
3. Toroidal Headers
4. Poloidal Headers and Connectors
5. Radial Flow Cells
6. S. S. Reflector
7. Shield
8. Divertor Slots
9. Superconducting Magnets

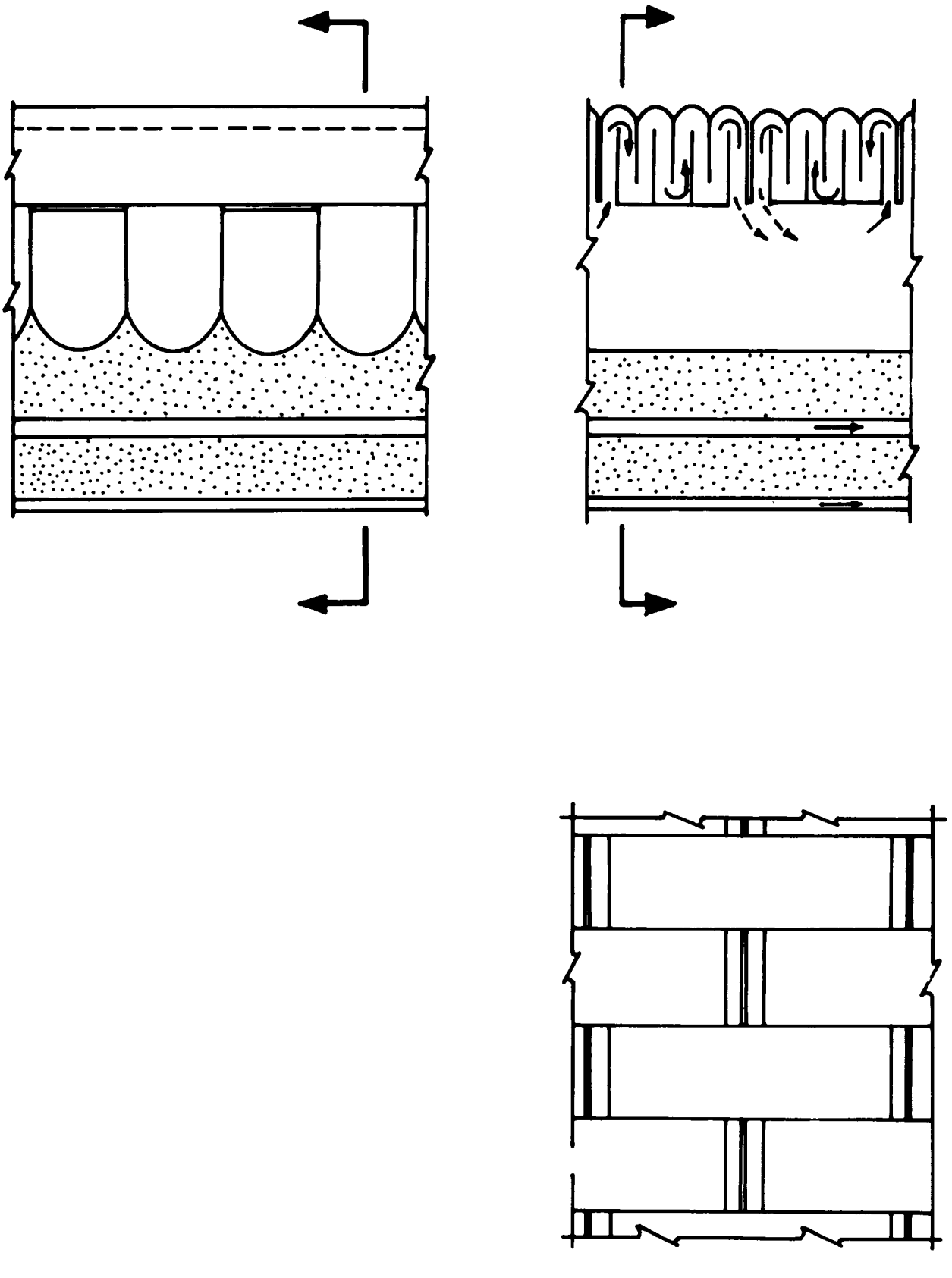

FIG. 2 SECTION VIEWS OF BLANKET

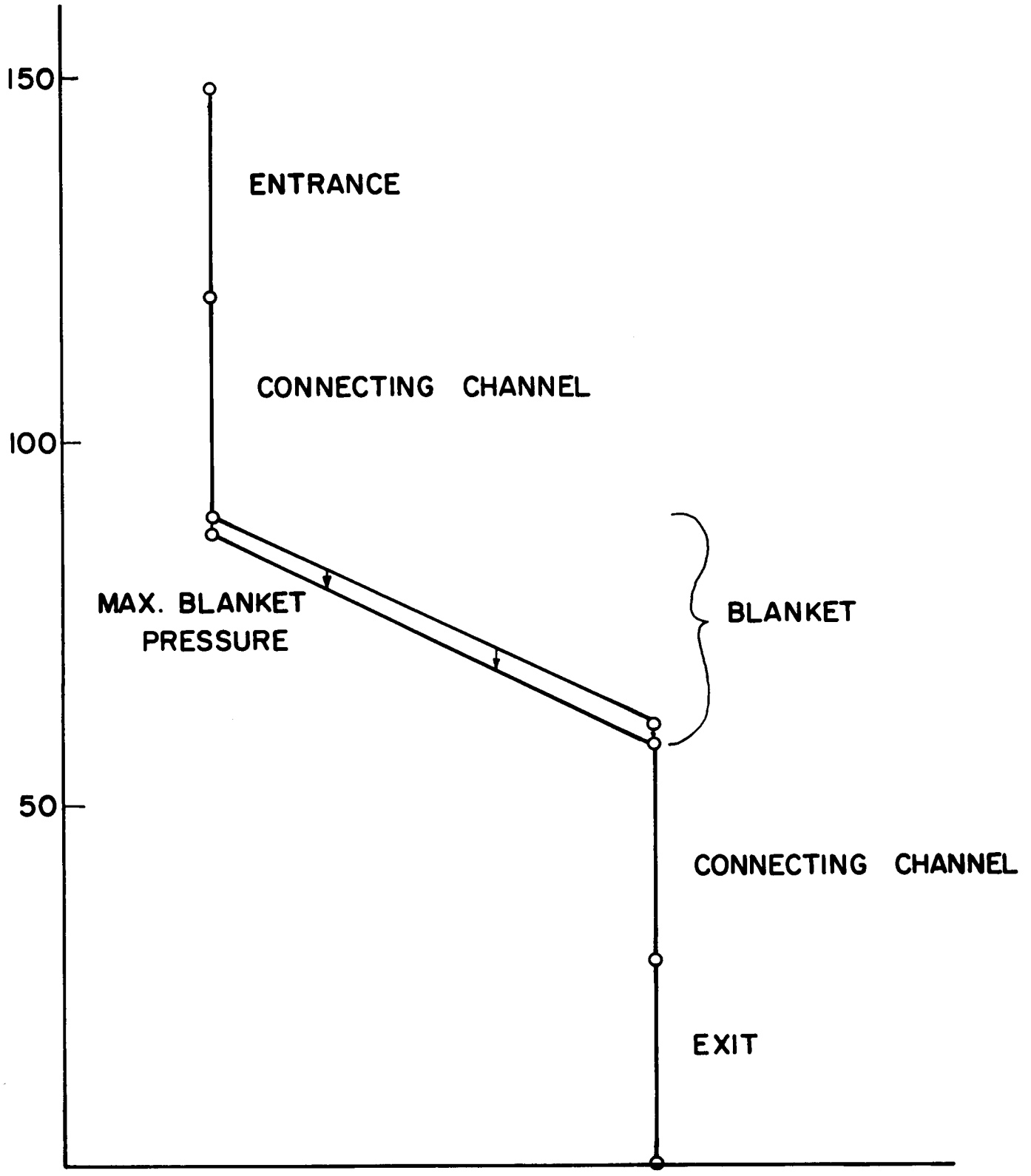

FIGURE 3 - Coolant Temperature Distribution

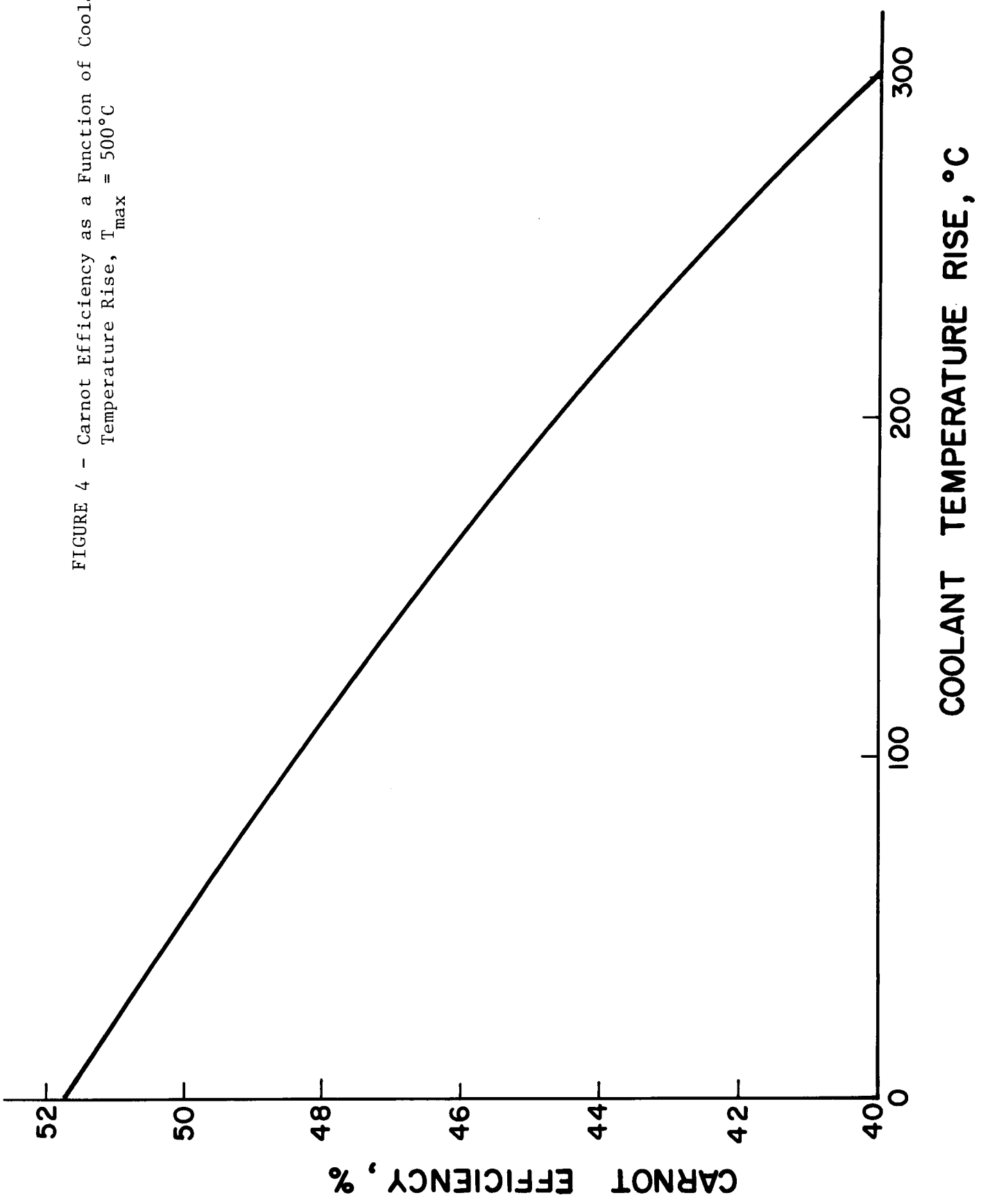

FIGURE 4 - Carnot Efficiency as a Function of Coolant Temperature Rise, T_{max} = 500°C